

Plasmon lifetime enhancement in a bright-dark mode coupled system

Bilge Can Yildiz,^{1,2,3,*} Alpan Bek,¹ and Mehmet Emre Tasgin²

¹*Department of Physics, Middle East Technical University, 06800 Ankara, Turkey*

²*Institute of Nuclear Sciences, Hacettepe University, 06800 Ankara, Turkey*

³*Faculty of Engineering and Natural Sciences, Photonics Laboratory, Tampere University, 33720 Tampere, Finland*

(Dated: May 21, 2019)

Metallic nanoparticles can localize the incident light to hotspots as plasmon oscillations, where the intensity can be increased up to four orders of magnitude. Even though the lifetime of plasmons are typically short, it can be increased via interactions with quantum emitters, e.g. spaser nanolasers. However, molecules can bleach in days. Here, we study the lifetime enhancement of plasmon excitations due to the coupling with longer lifetime dark plasmon modes. Exact solutions of the 3D Maxwell equations, i.e. FDTD, demonstrates that the lifetime of the coupled system increases, as also predicted by a basic oscillator model. We report an optimum bright-dark plasmon mode coupling, where lifetime enhancement becomes maximum, and show that no precise positioning of the nanostructures is required to obtain enhanced lifetime.

I. INTRODUCTION

Generation of strong local electromagnetic fields at the nanoscale is one of the major objectives in plasmonics. Resonant interaction of metal nanostructures (MNSs) with incident optical light provides localization of electromagnetic fields with up to ten thousand times higher intensity as compared to the incident field [1]. Achieving large electromagnetic field enhancements opens up development of fundamentally new metal-based subwavelength optical elements with broad technological potential in biological sensing [2–4], optical nanoantennas [5–7], subwavelength optical imaging [8–10], fluorescence enhancement [11–15], plasmonic metamaterials [16–18], and nonlinear plasmonics [19–21]. Despite remarkably enhanced amplitude, plasmon lifetime is typically short, most importantly due to radiative damping for MNSs larger than 20 nm [22]. Lifetime of localized surface plasmons have been of interest in recent years [23–26].

Noginov et. al. 2009, demonstrate a narrowing in the emission spectrum of a gold nanoparticle core, placed in a dye-doped silica shell [27]. Coupling between the gold nanoparticle and the dye molecules enables the system to respond with a decay rate of the molecular excited level, as a result of resonant energy transfer from excited molecules to surface plasmons. Lifetime extension due to coupling between plasmonic oscillators and quantum emitters is also theoretically demonstrated [28], where the path interference effects are utilized. In plasmonic solar cell applications, improved lifetime of plasmons play a very important role on the device efficiency, as light is carried along the photovoltaic structure for longer durations. On the other hand, obtaining lifetime enhancement without using quantum structures would simplifies fabrication. Quantum emitters are not as convenient as larger particles in the range from a few to a few hundred nanometers to be used in optical systems [29]. Besides,

molecules have limited exposure times. Instead of an atomic state, a dark plasmonic state could be advantageous in the sense that interaction between a plasmonic mode and an atom cannot be as strong as interaction between two plasmonic modes, due to their overlapping of the spatial extensions.

We investigate the effects of coupling between dark and bright plasmon modes to the plasmon lifetime. We consider a system of two MNSs, one of which supports a plasmonic dark state. A plasmonic dark state is a long-lived excitation that cannot be excited by linearly polarized field, but can couple to (be excited by) near-field polarization of an excited bright plasmon mode [30, 31]. When a system consists of plasmonic structures with modes resonant to a source field, this field can be confined into nanoscale dimensions, and interact with long-lived dark states. We consider such a system, schematized in Fig. 1, where the two plasmonic oscillators are coupled. Although we consider here a scheme where the dark mode belongs to a second MNS to simplify the FDTD simulations, the dark mode could also belong to the same MNS.

In this paper, we apply an analytical theoretical model based on harmonic oscillators, describing the oscillation dynamics of the two coupled plasmon modes. We demonstrate that the lifetime of the coupled system is enhanced compared to the uncoupled one, and the enhancement is the highest at an optimum phenomenological coupling constant, f , which is related with the distance between the two plasmonic structures. We numerically monitor the decay of the near field of the coupled system for a range of inter-structure distance by finite difference time domain (FDTD) [32] method. The lifetime of the system for changing values of the inter-structure distance exhibits a similar behavior to the one obtained by the theoretical model.

II. ANALYTICAL MODEL

The model system consists of two interacting harmonic oscillators, corresponding to two plasmon modes, sup-

* bilge.yildizkarakul@tuni.fi

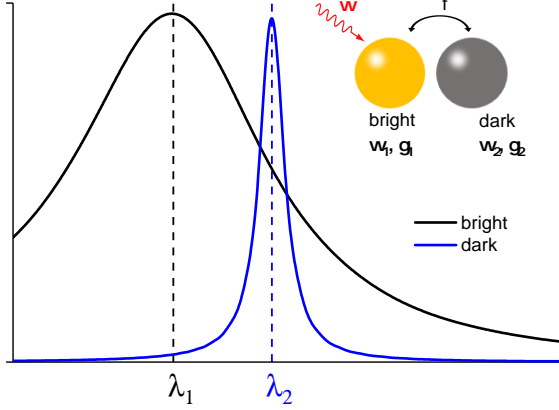


FIG. 1. Description of the coupled plasmon system. The graph shows representative optical responses of the MNSs.

ported by the two interacting MNSs, in the weak coupling regime. One of the MNSs supports a bright plasmon mode that is resonantly excited by the incident harmonic field. The lifetime of this driven plasmon mode is typically short. The second MNS supports a dark plasmon mode, which can be considered a quadrupole (or higher order) plasmon mode of an MNS. Dark plasmon modes cannot be excited by the incident harmonic field and are typically long-lived. When the two MNSs are brought together, the near field of the driven MNS excites the dark plasmon mode of the second MNS and the overall system displays hybridized plasmon resonances with modified lifetimes. The uncoupled driven and the dark plasmon modes are described by amplitudes $\alpha_i^{(0)}$, and associated with natural frequencies ω_i , and damping rates, γ_i , where $i = 1, 2$, respectively. The uncoupled eigenmodes are

$$\alpha_i^{(0)}(t) \propto e^{-(i\omega_i + \gamma_i)t}. \quad (1)$$

The total number of plasmons of the system, in the absence of coupling is determined by $\alpha_1^{(0)}(t)$, since the other mode is not excited without coupling. When the two particles are brought together, the modes are hybridized and there are contributions from the oscillations on both of the particles. The interaction between the oscillators is defined by a parameter f , in the dimension of frequency. The model is dimensionless, assuming the frequency of the pump field, $\omega = 1$. That follows, the damping rates and the coupling parameter, f , are treated as a factor of ω , and the time as a factor of $1/\omega$, which is also 1. A nonzero f corresponds to a case when the two MNSs are brought together; close enough for the polarization fields induced on the structures to overlap and hence interact.

The interaction between particles is expected to introduce path interferences at certain frequencies. When

there is a nonzero coupling between the structures, the solutions of the oscillations are hybridized [33]; being in the form of linear combinations of the two new oscillation modes, as,

$$\alpha_i(t) \propto e^{h_{i,1}} + e^{h_{i,2}}, \quad (2)$$

where functions appearing on the exponents are functions of the oscillation parameters, i.e., $h = h(\omega_1, \omega_2, \gamma_1, \gamma_2, f, t)$. The total number of plasmons in the coupled system is defined as,

$$N(t) = |\alpha_1(t)|^2 + |\alpha_2(t)|^2. \quad (3)$$

The lifetime of the induced plasmon oscillations, τ , can be defined as the mean value of the time weighted over plasmon intensity, as follows,

$$\tau = \frac{\int_0^\infty tN(t)dt}{\int_0^\infty N(t)dt}. \quad (4)$$

To find an expression for the Eq. 4, we start with writing the Hamiltonian of the coupled system in the Heisenberg picture as follows,

$$\begin{aligned} \hat{H} = & \hbar\omega_1\hat{a}_1^\dagger\hat{a}_1 + \hbar\omega_2\hat{a}_2^\dagger\hat{a}_2 \\ & + \hbar(f\hat{a}_1^\dagger\hat{a}_2 + f^*\hat{a}_2^\dagger\hat{a}_1) + i\hbar(\hat{a}_1^\dagger\varepsilon_p e^{-i\omega t}), \end{aligned} \quad (5)$$

where \hat{a}_1 (\hat{a}_1^\dagger) and \hat{a}_2 (\hat{a}_2^\dagger) are the annihilation (creation) operators for the collective plasmon excitations in the driven and the attached oscillators, corresponding to bright and dark modes. Since properties like entanglement [34–36] are not of interest, they will soon represent the amplitudes of the associated plasmon oscillations ($\hat{a}_i \rightarrow \alpha_i$) and the problem will be reduced to a classical problem. f is the coupling matrix element between the polarization field induced by \hat{a}_1 and \hat{a}_2 . The first and the second terms on the right hand side of Eq. 5 are the energy operators of the two oscillation modes. The third term corresponds to the interaction energy, and the last term corresponds to the coupling of the pump to the driven oscillator, \hat{a}_1 .

Equations of motion for the coupled plasmon modes are obtained using the Heisenberg equation and the damping rates are plugged in. The driving force term is removed, since the decay time of the coupled system, where the driven oscillator is initiated from the excited state, is of the interest. The operators are replaced with their eigenvalues. The equations of motion describing the dynamics of the coupled plasmonic oscillator system are the following,

$$\dot{\alpha}_1 = -(i\omega_1 + \gamma_1)\alpha_1 - if\alpha_2, \quad (6)$$

$$\dot{\alpha}_2 = -if^*\alpha_1 - (i\omega_2 + \gamma_2)\alpha_2. \quad (7)$$

Equations 6 and 7 form the eigenvalue equation of the system, with the following eigenvalues, $\lambda_{1,2}$, and eigenvectors, $\alpha^{(1),(2)}$,

$$\lambda_{1,2} = \frac{1}{2}[-a - b \pm \sqrt{(a - b)^2 - 4f^2}], \quad (8)$$

$$\alpha^{(1),(2)} = \begin{pmatrix} \frac{-if}{\sqrt{f^2 + (a + \lambda_{1,2})^2}} \\ \frac{a + \lambda_{1,2}}{\sqrt{f^2 + (a + \lambda_{1,2})^2}} \end{pmatrix}, \quad (9)$$

where,

$$\begin{aligned} a &= (i\omega_1 + \gamma_1), \\ b &= (i\omega_2 + \gamma_2), \end{aligned} \quad (10)$$

and f is assigned to be real to reduce the degree of freedom with the purpose of obtaining the simplest and the quickest evidence of lifetime enhancement. The general solution is found as,

$$\begin{aligned} \alpha_1(t) &= C_1 \frac{-if}{\sqrt{f^2 + (a + \lambda_1)^2}} e^{\lambda_1 t} \\ &+ C_2 \frac{-if}{\sqrt{f^2 + (a + \lambda_2)^2}} e^{\lambda_2 t}, \end{aligned} \quad (11)$$

$$\begin{aligned} \alpha_2(t) &= C_1 \frac{a + \lambda_1}{\sqrt{f^2 + (a + \lambda_1)^2}} e^{\lambda_1 t} \\ &+ C_2 \frac{a + \lambda_2}{\sqrt{f^2 + (a + \lambda_2)^2}} e^{\lambda_2 t}, \end{aligned} \quad (12)$$

where C_1 and C_2 are the coefficients to be determined according to the initial conditions. For this problem, the incident field is introduced and drives the plasmonic mode that is supported by the MNS with shorter lifetime, and then it is turned off. It is assumed that, initially there are only α_1 oscillations. So the initial conditions are given by,

$$\alpha_1(0) = 1, \quad \alpha_2(0) = 0. \quad (13)$$

Applying the initial conditions given in Eq. 13, the solutions are found as,

$$\alpha_1(t) = \frac{a + \lambda_2}{\lambda_2 - \lambda_1} e^{\lambda_1 t} - \frac{a + \lambda_1}{\lambda_2 - \lambda_1} e^{\lambda_2 t}, \quad (14)$$

$$\begin{aligned} \alpha_2(t) &= -\frac{(a + \lambda_1)(a + \lambda_2)}{if(\lambda_2 - \lambda_1)} e^{\lambda_1 t} \\ &+ \frac{(a + \lambda_1)(a + \lambda_2)}{if(\lambda_2 - \lambda_1)} e^{\lambda_2 t}. \end{aligned} \quad (15)$$

Substituting these into Eq. 3, the lifetime of the system of the two coupled oscillators is obtained from the

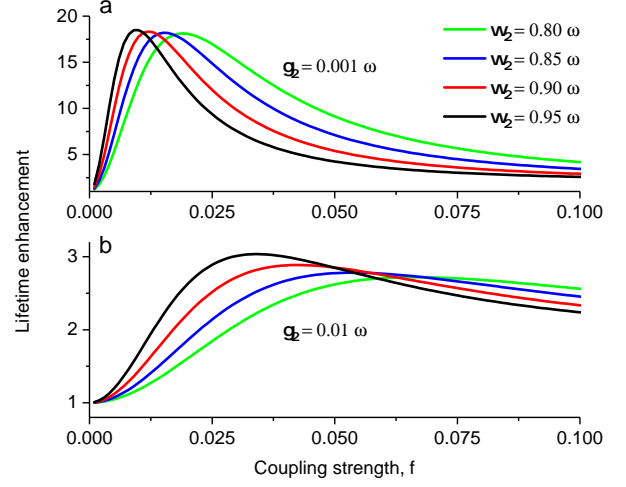


FIG. 2. Normalized lifetime of the coupled system, defined by Eq. 4, as a function of the coupling constant, f , for (a) $\gamma_2 = 0.001\omega$, and (b) $\gamma_2 = 0.01\omega$. In both cases; $\omega_1 = 1.0\omega$, and $\gamma_1 = 0.1\omega$.

analytical solutions of the integrations over time in Eq. 4. Figure 2 displays the lifetime enhancement with respect to the coupling strength, f , for several different $\omega_{1,2}$ and $\gamma_{1,2}$ sets. The lifetime enhancement is defined by the lifetime of the coupled system, that is calculated by Eq. 4, divided by the lifetime of the uncoupled system, where the MNS supporting dark plasmon mode is not present. In both calculations, the resonance frequency of the bright mode is $\omega_1 = 1.0$, and the damping rate $\gamma_1 = 0.1$. Curves with different colors show the cases where $\omega_2 = 0.80, 0.85, 0.90, 0.95$. In Fig. 2a, the damping rate of the dark mode is $\gamma_2 = 0.001$, and in Fig. 2b, it is $\gamma_2 = 0.01$.

We observe that when the ratio of the damping rates of the two plasmon modes is 100 (Fig. 2a), the maximum lifetime enhancement is achieved at $f = 0.01 - 0.02$ for different detunings ($\omega_1 - \omega_2$). When the ratio of the damping rates is 10 (Fig. 2b), the maximum lifetime enhancement is achieved at the higher values of f , that are $f = 0.03 - 0.06$, compared to the case shown in Fig. 2a. As the detuning of the resonance frequencies gets larger, stronger coupling is required to achieve the same lifetime enhancement, in both cases. The maximum lifetime enhancement is more than an order of magnitude in Fig. 2a, and it is around 3-fold in Fig. 2b. In both cases, f gets an optimum value. That means the lifetime of the coupled system is maximum for some optimum separation between the MNSs. For the values of f larger than its optimum, the lifetime enhancement saturates. This corresponds to a case where the MNSs are getting closer and closer. For all the values of f (inter-structure distance) smaller (larger) than its optimum, the lifetime enhancement exceeds unity, and it is unity when $f = 0$, that is when the MNSs are no longer coupled. Precise positioning of the MNSs is not required to enhance the

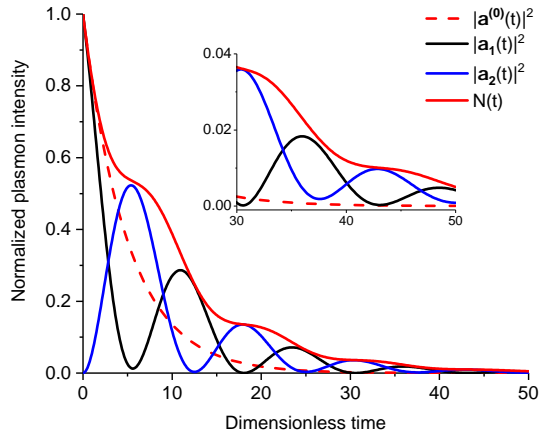


FIG. 3. Plasmon intensity for the uncoupled and coupled plasmon modes. In the inset, the axes are zoomed in a later time scale.

lifetime of the coupled system. These are the key outcomes of this work.

Figure 3 shows how the plasmon intensities decay in time, for coupled (solid curves) and uncoupled (dashed curve) cases. The horizontal axis is the dimensionless scalable time axis, where $t = 0$ represents the moment at which the incident pump pulse leaves the system. Since all parameters are scaled to the pump frequency, $\omega = 1$, dimensionless time can be calculated for its correspondence in SI units as follows: $t_{SI} = 1/\omega_{SI}$. For example if the pump frequency is $\omega = 2\pi \times 500$ THz, then 1 unit of dimensionless time corresponds to 0.32 fs. We note that the theoretical model does not encounter the physical sizes of the MNSs, hence does not encounter the retardation effects. Still, the time scale shown in Fig. 3 is consistent with the typical plasmon lifetime which is on the order of 1 – 100 fs, in the visible spectrum. Here we demonstrate the comparative decaying behavior of plasmon energy, for the coupled and uncoupled cases. Red solid (dashed) curve shows the normalized plasmon intensity in the coupled (uncoupled) cases. Absolute squares of the two coupled plasmon amplitudes are shown separately by black and blue curves. Inset graph shows the same, but zoomed in to the later times. For the uncoupled case, the number of plasmons in the system drops to zero at an earlier time. In the case of coupling, the energy of the system transfers back and forth intensely between the two modes at earlier times, and then dominantly localized on the attached MNS for later times.

III. FDTD SIMULATIONS

Next, we demonstrate the hybridization of the two plasmon modes. We realize the problem that we treat with our theoretical model, by considering two physical

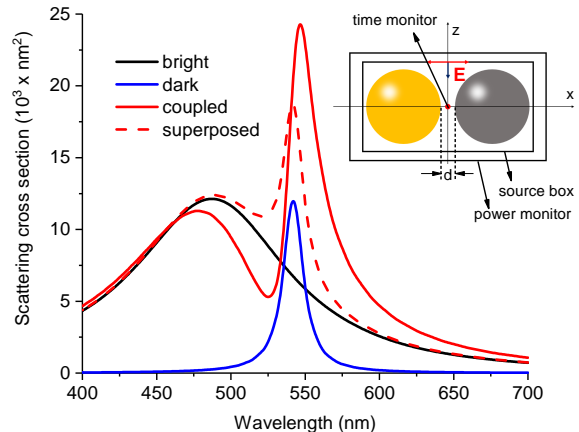


FIG. 4. Scattering cross section for the uncoupled and coupled plasmon modes, obtained by FDTD simulations. The inset shows the schematics of the simulation domain.

MNSs. For simplicity, we take the MNSs as nanospheres and describe their plasmonic resonances by Lorentz dielectric function. We set the Lorentz parameters of the two nanospheres so that each nanosphere supports single plasmon resonances which are overlapping, in their scattering cross section spectra. We set the damping rates of the two Lorentz dielectric functions such that the driven nanosphere's damping is 10 times larger than the other's. These two nanospheres can be considered as representative MNSs which are more complex in geometry. For example, the nanosphere with smaller damping can be considered as a metal nanorod with high aspect ratio, supporting higher order modes. Figure 4 demonstrates the hybridization between the plasmon modes of the two MNSs. We obtain the scattering cross sections of the MNSs by FDTD simulations in Lumerical FDTD Solutions. The size of MNSs are 100 nm and the separation between them is $d = 10$ nm. The source is a plane wave source which propagates along the z direction and polarized in the x direction, where the centers of the nanospheres are located (See inset of Fig. 4). Scattering cross section is calculated by a box power monitor, enclosing the associated nanospheres(s), which collects only the scattered power (excluding the source power). The boundaries of the simulation region are set to perfectly matched layers (PMLs) which absorbs the all the light incident upon. The scattering cross sections of individual MNSs are shown by black and blue curves, corresponding to the short- and long-lived plasmon modes. The resonance wavelengths are at 490 nm and 542 nm, for the short- and long-lived plasmon modes, respectively. The red dashed curve is obtained by adding the scattering cross sections of the two individual nanospheres. We compare this superposed response with the scattering cross section, computed for the case where the two MNSs are brought together. This coupled response is

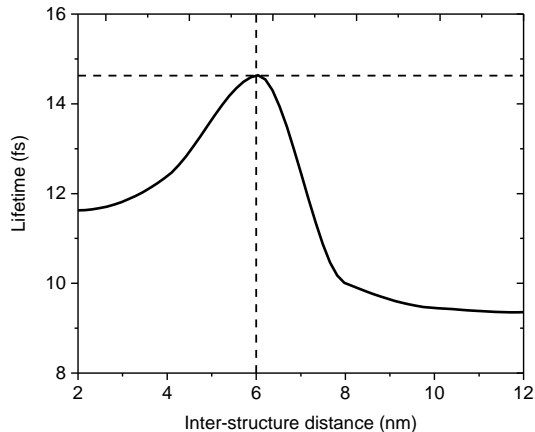


FIG. 5. Lifetime of the coupled system obtained by FDTD simulations.

shown by red solid curve. We observe that the individual resonances of the short and long-lived plasmon modes shift to the left and right, and get broader, and narrower, respectively. This demonstrates hybridization between individual plasmon modes, serving as a proof of electromagnetic interaction.

We now turn our attention to the question how the distance between the MNSs affects the interaction in terms of the lifetime of the coupled system. We construct a link between our theoretical models phenomenological coupling strength f , and the physical distance between the MNSs. We simulate how the electric fields decay in time for a range of inter-structure distance by a point monitor located at the hotspot of the coupled system (See inset of Fig. 4). The monitor location is kept fixed and the long-lifetime MNS is moved away from the other MNS step-wisely. The source is a plane wave with a very narrow spectrum, where the central wavelength is set to a slightly blue-detuned wavelength (480 nm) with respect to the resonance wavelength (490) of the short lifetime MNSs. In this way, the source excites only the MNS with short lifetime, and we observe the effect of the interaction between the MNSs for different inter-structure distances. After we obtain the intensity of the electric field recorded by the point monitor, as a function of time, we fit the simulation data to the exponential decay function, in the form of $I(t) = I_0 e^{-\tau/t}$, where τ is the lifetime of the oscillations. Figure 5 shows the lifetime obtained for different inter-structure distances. We observe that the lifetime of the system gets longer as the distance gets larger at first, reaches a maximum at a particular distance ($d = 6$ nm), and then starts to drop again. When the inter-structure distance is longer than ~ 50 nm, it drops down to 2.5 fs (not shown here), which is the lifetime of the isolated

short-lifetime MNS. This confirms the outcome of the theoretical model where the coupling strength, f , gets an optimum, and the normalized lifetime reaches to 1 when the MNSs are no longer coupled, at $f = 0$. For the nanostructures having resonance properties, shown in Fig. 4, the lifetime of the system can be enhanced by a factor of approximately 6, when their separation is 6 nm. Lifetime enhancement is also obtained at other inter-structure distances; hence, no precise positioning of the MNSs is required.

IV. DISCUSSION AND CONCLUSIONS

We examine the lifetime of a coupled plasmonic system of two MNSs, one of which can be excited by an incident field. The plasmon mode of the excited MNS has a large damping rate, i.e. a short lifetime. The second MNS has a longer lifetime but cannot be excited by the external field. Bringing two such MNSs together, so that they interact with each other, we demonstrate that it is possible to modify the decay properties of the overall system. Compared to the isolated MNS with shorter lifetime, coupled system decays much more slowly for a wide range of inter-structure distance. We examine the coupled system based on two different approaches. In the first approach, we apply a simple analytical model based on the solutions of the Heisenberg equation, where the MNSs are treated as size-less (point-like) harmonic oscillators, and the coupling between them is quantified by a phenomenological constant. This approach, which may appear like oversimplified, yields outcomes, in terms of the trend of the lifetime for varying coupling strengths similar to the results obtained by 3D solutions of the Maxwell's equations for finite-size MNSs. In the FDTD solutions, the retardation effects are fully accounted, and the coupling strength is quantified by the physical distance between the two MNSs. FDTD simulations show that as the distance between the MNSs gets smaller, lifetime increases up to a critical inter-structure distance. After this critical point, lifetime starts to decrease as the MNSs are brought even more closer, where strong hybridization starts. This behavior is similar to the observation of fluorescence enhancement near a MNSs [37]. Analogically, in the case of fluorescence enhancement, the fluorescent molecule is the long-lifetime object. We provide an extensive study on the lifetime of dark-bright plasmon modes, which would improve the current intuitive knowledge of the lifetime phenomenon. The results provide a deeper understanding of the classical mechanism of the coupling between two MNSs supporting bright and dark modes. The enhancement in the lifetime, obtained via coupling to a dark mode, offers implementations for technologies based on both linear and nonlinear response, e.g. solar cell and SERS, utilizing the plasmon localization.

- [1] M. I. Stockman, Nanoplasmonics: past, present, and glimpse into future, *Optics Express* **19**, 22029 (2011).
- [2] J. N. Anker, W. P. Hall, O. Lyandres, N. C. Shah, J. Zhao, and R. P. Van Duyne, Biosensing with plasmonic nanosensors, *Nature Materials* **7**, 442 (2008).
- [3] Y. Liu, Q. Liu, S. Chen, F. Cheng, H. Wang, and W. Peng, Surface Plasmon Resonance Biosensor Based on Smart Phone Platforms, *Scientific Reports* **5**, 12864 (2015).
- [4] J. R. Mejía-Salazar and O. N. Oliveira, Plasmonic Biosensing, *Chemical Reviews* **118**, 10617 (2018).
- [5] D. Dregely, R. Taubert, J. Dorfmueller, R. Vogelgesang, K. Kern, and H. Giessen, 3D optical Yagi-Uda nanoantenna array, *Nature Communications* **2**, 267 (2011).
- [6] G. M. Akselrod, C. Argyropoulos, T. B. Hoang, C. Ciraci, C. Fang, J. Huang, D. R. Smith, and M. H. Mikkelsen, Probing the mechanisms of large Purcell enhancement in plasmonic nanoantennas, *Nature Photonics* **8**, 835 (2014).
- [7] P. B. Savaliya, A. Thomas, R. Dua, and A. Dhawan, Tunable optical switching in the near-infrared spectral regime by employing plasmonic nanoantennas containing phase change materials, *Optics Express* **25**, 23755 (2017).
- [8] N. Fang, H. Lee, C. Sun, and X. Zhang, Sub-Diffraction-Limited Optical Imaging with a Silver Superlens, *Science* **308**, 534 (2005).
- [9] S. A. Maier, *Metamaterials and Imaging with Surface Plasmon Polaritons*, in *Plasmonics: Fundamentals and Applications* (Springer US, New York, NY, 2007) pp. 193–200.
- [10] S. Kawata, Y. Inouye, and P. Verma, Plasmonics for near-field nano-imaging and superlensing, *Nature Photonics* **3**, 388 (2009).
- [11] P. P. Pompa, L. Martiradonna, A. D. Torre, F. D. Sala, L. Manna, M. De Vittorio, F. Calabi, R. Cingolani, and R. Rinaldi, Metal-enhanced fluorescence of colloidal nanocrystals with nanoscale control, *Nature Nanotechnology* **1**, 126 (2006).
- [12] P. Bharadwaj and L. Novotny, Spectral dependence of single molecule fluorescence enhancement, *Optics Express* **15**, 14266 (2007).
- [13] S. Y. Liu, L. Huang, J. F. Li, C. Wang, Q. Li, H. X. Xu, H. L. Guo, Z. M. Meng, Z. Shi, and Z. Y. Li, Simultaneous excitation and emission enhancement of fluorescence assisted by double plasmon modes of gold nanorods, *Journal of Physical Chemistry C* **117**, 10636 (2013).
- [14] F. Carreño, M. A. Antón, V. Yannopapas, and E. Paspalakis, Resonance fluorescence spectrum of a Λ -type quantum emitter close to a metallic nanoparticle, *Physical Review A* **94**, 013834 (2016).
- [15] L.-Y. Hsu, W. Ding, and G. C. Schatz, Plasmon-Coupled Resonance Energy Transfer, *The Journal of Physical Chemistry Letters* **8**, 2357 (2017).
- [16] F. J. Garcia-Vidal, L. Martín-Moreno, and J. B. Pendry, Surfaces with holes in them: new plasmonic metamaterials, *Journal of Optics A: Pure and Applied Optics* **7**, S97 (2005).
- [17] N. I. Zheludev, A Roadmap for Metamaterials, *Optics and Photonics News* **22**, 30 (2011).
- [18] G. V. Naik, V. M. Shalae, and A. Boltasseva, Alternative Plasmonic Materials: Beyond Gold and Silver, *Advanced Materials* **25**, 3264 (2013).
- [19] S. Kawata, Plasmonics for Nanoimaging and Nanospectroscopy, *Applied Spectroscopy* **67**, 117 (2013).
- [20] J. Zhang, J. Li, S. Tang, Y. Fang, J. Wang, G. Huang, R. Liu, L. Zheng, X. Cui, and Y. Mei, Whispering-gallery nanocavity plasmon-enhanced Raman spectroscopy, *Scientific Reports* **5**, 1 (2015).
- [21] V. P. Drachev, A. V. Kildishev, J. D. Borneman, K.-P. Chen, V. M. Shalae, K. Yamnitskiy, R. A. Norwood, N. Peyghambarian, S. R. Marder, L. A. Padilha, S. Webster, T. R. Ensley, D. J. Hagan, and E. W. Van Stryland, Engineered nonlinear materials using gold nanoantenna array, *Scientific Reports* **8**, 780 (2018).
- [22] A. Melikyan and H. Minassian, On surface plasmon damping in metallic nanoparticles, *Applied Physics B* **78**, 453 (2004).
- [23] A. S. Kirakosyan, M. I. Stockman, and T. V. Shahbazyan, Surface plasmon lifetime in metal nanoshells, *Physical Review B* **94**, 155429 (2016).
- [24] G. D. Mahan, Lifetime of surface plasmons, *Physical Review B* **97**, 075405 (2018).
- [25] M. Di Vece, Very Long Plasmon Oscillation Lifetimes in the Gap Between Two Gold Particles, *Plasmonics* **13**, 1367 (2018).
- [26] K. D. Chapkin, L. Bursi, G. J. Stec, A. Lauchner, N. J. Hogan, Y. Cui, P. Nordlander, and N. J. Halas, Lifetime dynamics of plasmons in the few-atom limit., *Proceedings of the National Academy of Sciences of the United States of America* **115**, 9134 (2018).
- [27] M. A. Noginov, G. Zhu, A. M. Belgrave, R. Bakker, V. M. Shalae, E. E. Narimanov, S. Stout, E. Herz, T. Suteewong, and U. Wiesner, Demonstration of a spaser-based nanolaser, *Nature* **460**, 1110 (2009).
- [28] M. E. Tagn, Metal nanoparticle plasmons operating within a quantum lifetime, *Nanoscale* **5**, 8616 (2013).
- [29] M. I. Stockman, Dark-hot resonances, *Nature* **467**, 541 (2010).
- [30] D. E. Gómez, Z. Q. Teo, M. Altissimo, T. J. Davis, S. Earl, and A. Roberts, The Dark Side of Plasmonics, *Nano Letters* **13**, 3722 (2013).
- [31] S. Panaro, A. Nazir, C. Liberale, G. Das, H. Wang, F. De Angelis, R. Proietti Zaccaria, E. Di Fabrizio, and A. Toma, Dark to Bright Mode Conversion on Dipolar Nanoantennas: A Symmetry-Breaking Approach, *ACS Photonics* **1**, 310 (2014).
- [32] A. Taflove and S. C. Hagness, *Computational electrodynamics: the finite-difference time-domain method* (Artech House, 2005) p. 1006.
- [33] P. Nordlander, C. Oubre, E. Prodan, K. Li, and M. I. Stockman, Plasmon Hybridization in Nanoparticle Dimers 10.1021/NL049681C (2004).
- [34] Q. Sun, M. Al-Amri, A. Kamli, and M. S. Zubairy, Lamb shift due to surface plasmon polariton modes, *Physical Review A* **77**, 062501 (2008).
- [35] V. Yannopapas, E. Paspalakis, and N. V. Vitanov, Plasmon-Induced Enhancement of Quantum Interference near Metallic Nanostructures, *Physical Review Letters* **103**, 063602 (2009).

- [36] M. Qurban, M. Ikram, G.-Q. Ge, and M. S. Zubairy, Entanglement generation among quantum dots and surface plasmons of a metallic nanoring, *Journal of Physics B: Atomic, Molecular and Optical Physics* **51**, 155502 (2018).
- [37] P. Anger, P. Bharadwaj, and L. Novotny, Enhancement and Quenching of Single-Molecule Fluorescence, *Physical Review Letters* **96**, 113002 (2006).